

See discussions, stats, and author profiles for this publication at: <https://www.researchgate.net/publication/7881215>

# Morphiceptin Analogues Containing a Dipeptide Mimetic Structure: An Investigation on the Bioactive Topology at the $\mu$ -Receptor

ARTICLE in JOURNAL OF MEDICINAL CHEMISTRY · JUNE 2005

Impact Factor: 5.45 · DOI: 10.1021/jm040867y · Source: PubMed

CITATIONS

16

READS

17

10 AUTHORS, INCLUDING:



**Paolo Grieco**

University of Naples Federico II

177 PUBLICATIONS 2,342 CITATIONS

SEE PROFILE



**Pietro Campiglia**

Università degli Studi di Salerno

143 PUBLICATIONS 1,326 CITATIONS

SEE PROFILE



**Vincenzo Calderone**

Università di Pisa

139 PUBLICATIONS 1,824 CITATIONS

SEE PROFILE



**Isabel M Gomez-Monterrey**

University of Naples Federico II

99 PUBLICATIONS 1,935 CITATIONS

SEE PROFILE

## Morphiceptin Analogues Containing a Dipeptide Mimetic Structure: An Investigation on the Bioactive Topology at the $\mu$ -Receptor

Paolo Grieco,<sup>#</sup> Laura Giusti,<sup>§</sup> Alfonso Carotenuto,<sup>#</sup> Pietro Campiglia,<sup>#</sup> Vincenzo Calderone,<sup>§</sup> Teresa Lama,<sup>#</sup> Isabel Gomez-Monterrey,<sup>#</sup> Gianpaolo Tartaro,<sup>‡</sup> Maria R. Mazzoni,<sup>§</sup> and Ettore Novellino<sup>\*,#</sup>

*Dipartimento di Chimica Farmaceutica e Tossicologica, Università degli Studi di Napoli "Federico II", I-80131 Napoli, Italy, Dipartimento di Psichiatria, Neurobiologia, Farmacologia e Biotecnologie, Università di Pisa, Pisa, Italy and Dipartimento di Patologia Testa, Collo, Cavo Orale e Comunicazione Audio Verbale, Seconda Università di Napoli, Napoli, Italy*

Received July 29, 2004

We describe the design, the conformational behavior, and the biological activity at the  $\mu$ -opioid receptor of new morphiceptin analogues. In these analogues a recently described dipeptide mimetic structure replaces both the N- and the C-terminal Xaa-Pro dipeptide of morphiceptin. Conformational investigation on the most active analogue, compared to the parent peptide, indicates a high degree of structural tolerance within the  $\mu$ -opioid receptor binding site. In fact, our results indicate that only the location and the relative orientation of the side chains of the aromatic pharmacophoric residues represent the indispensable structural features for  $\mu$ -receptor binding. To reach such topological arrangement, opioid peptides can adopt different conformations and configurations. In particular, opioid peptides bearing a proline residue as spacer between the two aromatic residues can adopt, in the active state, both *cis* and *trans* configurations at the Tyr<sup>1</sup>-Pro<sup>2</sup> amide bond, each of them with the appropriate backbone and side chains orientations.

### Introduction

Opioids have always attracted increasing research interest primarily for their powerful pain relieving properties and their potential for recreational abuse. Opioids exert their biological actions through three types of receptors, identified as  $\mu$ ,  $\kappa$ , and  $\delta$ .<sup>1,2</sup> Development of both peptide<sup>3</sup> and nonpeptide<sup>4</sup> selective receptor ligands and the recent cloning of opioid receptors have provided efficient tools for the functional studies of these receptors. In particular, experiments of  $\mu$ -opioid receptor knockout mice have demonstrated that this receptor mediates most of the opioid actions, including analgesia, tolerance, and reward.<sup>5</sup> Therefore, selective ligands for this receptor subtype could be very useful as drug candidates.

Many natural and synthetic opioid tetrapeptides show both high affinity and specificity for  $\mu$ -receptor. In this context, morphiceptin (H-Tyr-Pro-Phe-Pro-NH<sub>2</sub>)<sup>6</sup> and the endomorphins [endomorphin-1 (H-Tyr-Pro-Trp-Phe-NH<sub>2</sub>) and endomorphin-2 (H-Tyr-Pro-Phe-Phe-NH<sub>2</sub>)]<sup>7</sup> are opioid peptide agonists with high selectivity for  $\mu$  opioid receptors. These peptides contain a Pro residue in position 2, and consequently *cis/trans* isomerization occurs at the Tyr<sup>1</sup>-Pro<sup>2</sup> peptide bond.<sup>8–10</sup> In fact, previous results of <sup>1</sup>H NMR spectroscopic studies performed on morphiceptin and endomorphins in aqueous and DMSO solutions indicated the existence of a *cis/trans* equilibrium with a predominance of the *trans* isomer in all cases.<sup>8–11</sup> The *cis/trans* configuration around the

Tyr<sup>1</sup>-Pro<sup>2</sup> amide bond is of particular significance for morphiceptin and endomorphins bioactivity because this bond is located within the biologically important N-terminal tripeptide message sequence.<sup>12</sup> To elucidate the active configuration around this peptide bond, extensive conformational studies have been performed on the endogenous peptides morphiceptin, endomorphins, and their analogues.<sup>8–11,13–18</sup> Briefly, while for morphiceptin there is general consensus about a Pro<sup>2</sup> *cis* configuration in the bioactive structure,<sup>14</sup> Pro<sup>2</sup> configuration in endomorphin-1 bioactive structure has been reported both as *trans*<sup>9,15</sup> and *cis*.<sup>11</sup> Similarly, endomorphin-2 active derivatives were shown to possess both *trans*<sup>17</sup> and *cis*<sup>16,18</sup> configuration. Furthermore, morphiceptin has a second proline residue at position 4; therefore, the *cis/trans* isomerization occurs at both Tyr<sup>1</sup>-Pro<sup>2</sup> and Phe<sup>3</sup>-Pro<sup>4</sup> peptide bonds.<sup>8</sup>

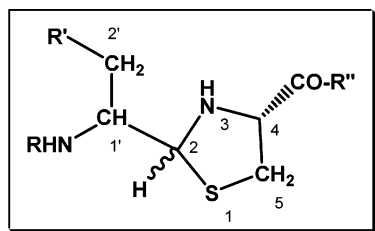
In an attempt to obtain additional information on the importance of *cis/trans* isomerization at proline peptide bonds of morphiceptin and on the overall structural requirements of  $\mu$ -opioid selective ligands, we synthesized and biologically evaluated new analogues in which a previously reported dipeptide mimetic structure<sup>19</sup> has been introduced in the peptide sequence (Figure 1). Since in this dipeptide mimetic the amide bond is replaced by a single rotatable bond between the C-1' and the C-2 atom of the *pseudo*-dipeptide, no *cis-trans* isomerization can occur. We replaced, one by one, both the N- and the C-terminal Xaa-Pro dipeptide of morphiceptin with the corresponding dipeptide mimetic obtaining the compounds **2** and **3**, respectively (Figure 1). Successively, following the biological results which indicate that only the replacement of the C-terminal dipeptide is tolerated at the  $\mu$ -opioid receptor, we tested two further analogues in which the *pseudo*-Phe residue of **3** was replaced with a *pseudo*-D-Phe or a *pseudo*-Trp

\* Corresponding author: Prof. Ettore Novellino, Dipartimento di Chimica Farmaceutica e Toss., Università di Napoli "Federico II", Via D. Montesano, 49, 80131, Napoli, Italy. Phone: +39-081-678646, Fax: +39-081-678644, e-mail: novellino@unina.it.

<sup>#</sup> Università degli Studi di Napoli "Federico II".

<sup>§</sup> Università di Pisa.

<sup>‡</sup> Seconda Università di Napoli.



|   | R        | R'  | R''                      | Conf. C1' |
|---|----------|-----|--------------------------|-----------|
| 2 | H-       | HO- | -Phe-Pro-NH <sub>2</sub> | (S)       |
| 3 | Tyr-Pro- |     | -NH <sub>2</sub>         | (S)       |
| 4 | Tyr-Pro- |     | -NH <sub>2</sub>         | (R)       |
| 5 | Tyr-Pro- |     | -NH <sub>2</sub>         | (S)       |

**Figure 1.** Structures of morphiceptin analogues analyzed in the present study. The dipeptide mimetic structure has been highlighted.

residue leading to the compounds **4** and **5**, respectively. Finally, conformational preferences of the most active compound **3** and of the parent morphiceptin **1** were elucidated by <sup>1</sup>H NMR spectroscopy in a membrane mimetic environment.

## Results

**Chemistry.** The dipeptide mimetics were synthesized by a modified Schmidt procedure as we previously reported.<sup>19</sup> Briefly, the starting Fmoc-(Tyr, or Phe, or D-Phe, or Trp)-H, prepared from the corresponding Fmoc-amino acid by reduction of its *N,O*-dimethylhydroxamate derivatives, was added to cysteine hydrochloride in the presence of potassium hydrogen carbonate to provide the thiazolidine derivatives. The resulting compound mimics a dipeptide with a *pseudo*-aromatic residue in position 1 and a *pseudo*-proline (thiazolidine) in position 2 (Figure 1). Before introduction to the solid phase, the *pseudo*-dipeptide derivatives were N-Boc protected using classic methodology. <sup>1</sup>H NMR analysis of the crude products showed the presence of two stereoisomers in 4:1 ratio.

Final compounds were synthesized by the solid-phase approach using the standard Fmoc methodology in a manual reaction vessel<sup>20</sup> (See Experimental Section). The purification was achieved using a semipreparative RP-HPLC C 18 bonded silica column (Vydac 218TP1010). The purified compounds were 98% pure as determined by analytical RP-HPLC. The correct molecular weight of the compounds was confirmed by mass spectrometry and amino acid analysis. The analytical data for each compound are presented in Table 1.

**Biological Activity.** Compound biological activity was tested both in binding and functional assays. Inhibition of [<sup>3</sup>H]DAMGO binding to rat brain membranes was evaluated at various compound concentrations. The concentration–response curves were analyzed and compared to the inhibition curve obtained for morphiceptin (Figure 2, panel A). Derived *K<sub>i</sub>* values are reported in Table 2. In functional assays, inhibition of

**Table 1.** Physicochemical Properties of the Compounds 2–5

| compd | solvent<br>A <sup>a</sup> | solvent<br>B <sup>a</sup> | solvent<br>C <sup>a</sup> | MW     | MS     | HPLC <sup>b</sup> |
|-------|---------------------------|---------------------------|---------------------------|--------|--------|-------------------|
| 2     | 0.77                      | 0.06                      | 0.46                      | 511.64 | 511.93 | 3.89              |
| 3     | 0.82                      | 0.05                      | 0.44                      | 511.64 | 511.96 | 3.51              |
| 4     | 0.78                      | 0.07                      | 0.40                      | 511.64 | 511.91 | 3.93              |
| 5     | 0.88                      | 0.06                      | 0.49                      | 550.67 | 550.78 | 3.41              |

<sup>a</sup> Solvent systems: (A) 1-butanol/HOAc/pyridine/H<sub>2</sub>O (5:5:1:4); (B) EtOAc/pyridine/AcOH/H<sub>2</sub>O (5:5:1:3); (C) 1-butanol/AcOH/H<sub>2</sub>O (4:1:1). <sup>b</sup> Analytical HPLC performed on a C18 column (Vydac 218TP104) using a gradient of acetonitrile in 0.1% aqueous TFA at 1 mL/min. The following gradient was used: 10–90% acetonitrile in 40 min.

**Table 2.** Values of *K<sub>i</sub>* (nM) and EC<sub>50</sub> (nM) Recorded in [<sup>3</sup>H]DAMGO Binding and Functional Experiments

| compd | [ <sup>3</sup> H]DAMGO binding:<br><i>K<sub>i</sub></i> (nM)<br>(mean ± SEM) | functional assay         |                                       |
|-------|--|--------------------------|---------------------------------------|
|       |  | efficacy<br>(mean ± SEM) | EC <sub>50</sub> (nM)<br>(mean ± SEM) |
| 1     | 25.6 ± 4 ( <i>n</i> = 4)   | 65 ± 8 ( <i>n</i> = 4)   | 13 ± 11 ( <i>n</i> = 4)               |
| 2     | 3100 ± 200 ( <i>n</i> = 3)   | 17 ± 6 ( <i>n</i> = 4)   | not calculable <sup>a</sup>           |
| 3     | 14.1 ± 1 ( <i>n</i> = 4)   | 65 ± 9 ( <i>n</i> = 6)   | 9.7 ± 2.6 ( <i>n</i> = 6)             |
| 4     | 290 ± 46 ( <i>n</i> = 3)   | 71 ± 4 ( <i>n</i> = 5)   | 36 ± 14 ( <i>n</i> = 5)               |
| 5     | 178 ± 17 ( <i>n</i> = 4)   | 70 ± 5 ( <i>n</i> = 6)   | 28 ± 8 ( <i>n</i> = 6)                |

<sup>a</sup> The parameter could not be calculated because of the low efficacy. *n*: number of experiments.

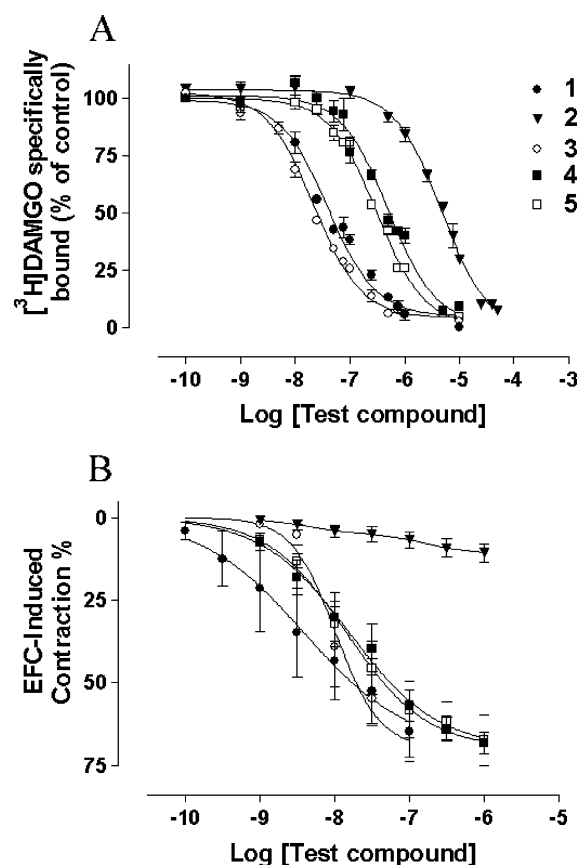


**Figure 2.** Curves relative to (A) effects of compounds on inhibition of [<sup>3</sup>H]DAMGO binding to rat brain membranes; (B) inhibition of EFS-induced contractile responses of guinea-pig ileum. Vertical bars indicated SEM.

isolated guinea pig ileum contraction induced by electrical stimulation was investigated. The inhibitory effects of various concentrations of tested compounds were compared to those obtained using known opioid receptor agonists, such as DAMGO, loperamide, and morphine. The maximal efficacy of all three agonists was ap-

**Table 3.**  $^1\text{H}$  NMR Resonance Assignments<sup>a</sup> of Analyzed Compounds in SDS- $d_{25}$  200 mM Solution

| residue <sup>b</sup>     | NH ( $^3J_{\text{N}\alpha}$ , ex, Tc) <sup>c</sup> | C $^{\alpha}\text{H}$ ( $^3J_{\alpha\beta}$ ) <sup>c</sup> | C $^{\beta}\text{H}$ | others   |
|--------------------------|--|--|----------------------|--|
| <b>3a</b>                |  |  |                      |  |
| Tyr <sup>1</sup>         |  | 4.46 (4.0, 10.8)   | 3.19, 3.00           | 7.23 ( $\delta$ ); 6.89 ( $\epsilon$ )                   |
| Pro <sup>2</sup>         |  | 4.35 (4.6, 7.6)  | 1.88, 1.13           | 1.84, 1.66 ( $\gamma$ ); 3.79, 3.39 ( $\delta$ )         |
| $\psi$ -Phe <sup>3</sup> | 7.77 (4.5, s, 2.7)                                 | 3.98 (10.5, 4.5)   | 3.34, 3.03           | 7.17 ( $\delta$ ); 7.21 ( $\epsilon$ )                   |
| Thiaz                    |  |  |                      | 5.58 (C-2); 4.94 (C-4); 3.82, 3.42 (C-5) 7.24 ( $\eta$ ) |
| <b>1 all-trans</b>       |  |  |                      |  |
| Tyr <sup>1</sup>         |  | 4.39 (6.8, 7.0)  | 2.88                 | 7.06 ( $\delta$ ); 6.79 ( $\epsilon$ )                   |
| Pro <sup>2</sup>         |  | 4.54 (3.6, 8.2)  | 2.06, 1.87           | 1.90, 1.72 ( $\gamma$ ); 3.67, 3.07 ( $\delta$ )         |
| Phe <sup>3</sup>         | 7.50 (7.2, f, 6.0)                                 | 4.82 (9.0, 5.5)  | 3.16, 3.01           | 7.28 ( $\delta$ ); 7.26 ( $\epsilon$ )                   |
| Pro <sup>4</sup>         |  | 4.35 (4.6, 8.7)  | 2.22, 1.90           | 1.86 ( $\gamma$ ); 3.71, 3.31 ( $\delta$ )               |
| <b>1 cis-trans</b>       |  |  |                      |  |
| Tyr <sup>1</sup>         |  | 3.50 (10.5, 4.5)   | 2.99, 2.87           | 6.91 ( $\delta$ ); 6.76 ( $\epsilon$ )                   |
| Pro <sup>2</sup>         |  | 3.13 (5.1, 7.2)  | 1.64                 | 1.51, 1.35 ( $\gamma$ ); 3.42, 3.27 ( $\delta$ )         |
| Phe <sup>3</sup>         | 8.00 (7.2, f, 6.5)                                 | 4.86 (10.3, 5.2)   | 3.23, 2.95           | 7.34 ( $\delta$ ); 7.32 ( $\epsilon$ )                   |
| Pro <sup>4</sup>         |  | 4.31 (5.6, 9.2)  | 2.24                 | 1.95 ( $\gamma$ ); 3.81, 3.57 ( $\delta$ )               |

<sup>a</sup> Obtained at 300 K, pH = 5.5, with TSP ( $\delta$  0.00 ppm) as reference shift. Chemical shifts are accurate to  $\pm 0.02$  ppm. <sup>b</sup>  $\psi$ -Phe<sup>3</sup>: *pseudo*-Phe<sup>3</sup> and Thiaz: thiazolidine ring. <sup>c</sup>  $^3J$  coupling constants in Hz. ex = HN exchange rate (f, fast; s, slow). Tc =  $-\Delta\delta/\Delta T$  (ppb/K).

proximately 65% (efficacy,  $61 \pm 9$ ,  $68 \pm 11$ , and  $66 \pm 9\%$  for DAMGO, loperamide, and morphine, respectively). The  $\text{EC}_{50}$  values for DAMGO, loperamide, and morphine were  $36.2 \pm 11.1$ ,  $488.9 \pm 127.4$ , and  $30.7 \pm 11.2$  nM, respectively. Both loperamide and morphine inhibitions were antagonized by naloxone (data not shown). In Figure 2, panel B, the concentration-response curves of morphiceptin and synthesized compounds are shown while in Table 2 the derived  $\text{EC}_{50}$  values are compared to  $K_i$  values obtained from binding assays.

Replacement of Tyr<sup>1</sup>-Pro<sup>2</sup> with the new motif in compound **2** caused a dramatic decrease of drug potency in inhibiting [ $^3\text{H}$ ]DAMGO binding as indicated by 120-fold increase of the  $K_i$  value in comparison to that of morphiceptin. In functional studies, this compound did not produce any inhibition of ileum contraction within the concentration range tested. In contrast, the compound **3** in which Phe<sup>3</sup>-Pro<sup>4</sup> is replaced with the corresponding dipeptide mimetic structure was as active as morphiceptin both in binding and functional assays. In the last assay, the compound **3** showed an efficacy parameter comparable to that of the reference agonists, exhibiting the pharmacodynamic profile of full agonist. The activity as opioid receptor agonist of this compound was confirmed by the naloxone-induced reversibility of smooth muscle contraction inhibition (data not shown). Successively, keeping the dipeptide mimetic moiety at the C-terminal position, we replaced the *pseudo*-Phe residue of **3** with a *pseudo*-D-Phe or a *pseudo*-Trp residue, obtaining the compounds **4** and **5**, respectively (Figure 1). These substitutions are rationally supported by the observation that various morphiceptin analogues, in which the Phe<sup>3</sup> was replaced by other aromatic residues, preserve  $\mu$ -opioid activity.<sup>21</sup> Compounds **4** and **5** were 12- and 7-fold less potent inhibitors of [ $^3\text{H}$ ]DAMGO binding to membranes than morphiceptin. However, both these compounds were slightly less potent than morphiceptin in inhibiting ileum smooth muscle contraction with the pharmacological pattern of full agonists. The specificity of this effect through activation of opioid receptors was confirmed by naloxone antagonism (data not shown). The slight differences between  $K_i$  and  $\text{EC}_{50}$  values of these compounds might be the consequence of the use of tissue preparations obtained from different animal species.

**NMR Analysis.** A conformational analysis of morphiceptin and of the most active peptide **3** was performed using NMR and molecular modeling techniques. To date, many conformational studies have been performed to reveal the bioactive conformation of  $\mu$ -opioid peptides. However, the conformational flexibility of opioid peptides has hampered numerous attempts at determining the relationship between the solution conformation and activity using spectroscopic and modeling methods. It is known that the conformational space of the short opioid peptides is strongly affected by local environments<sup>22</sup> and that is generally poorly defined in aqueous solution. Since many hormones and neurotransmitters have been found to interact with the phospholipid bilayer and the resulting conformational preferences in the membrane-bound state have been correlated with their bioactivities,<sup>23</sup> we have determined the conformational preferences of **3** in SDS micelles and compared the results with those obtained for the parent peptide **1**.

**Compound 3 in SDS Micelles.** In the 1D  $^1\text{H}$  NMR spectrum of **3** in SDS micelles, four distinct sets of signals are detected which arise from the cis/trans isomerization of the Tyr-Pro peptide bond, and from the inversion of the C-2 chiral center of the thiazolidine ring (Figure 1). Integration of the signals in the 1D spectrum reveals the prevalence of one structure which accounts for 82% of all the isomers (the populations of the other isomers are about 7%, 7%, and 4% of the total). All the resonances of this major isomer (**3a**) were assigned following the Wüthrich procedure<sup>24</sup> via the usual systematic application of DQF-COSY,<sup>25</sup> TOCSY,<sup>26</sup> and NOESY<sup>27</sup> experiments with the support of the XEASY software package (Table 3).<sup>28</sup> Since only few signals unambiguously belong to the three minor isomers, complete assignment and structure determination were not possible in these cases. Partial assignment of the  $^1\text{H}$  NMR resonances of the three minor isomers is reported in the Supporting Information (isomers **3b**–**d**). The following descriptions will be focused on the major solution isomer **3a**.

Sequential NOE connectivities of the Tyr<sup>1</sup> H $\alpha$  with the Pro<sup>2</sup> H $\delta$ 's evidence that Tyr-Pro peptide bond has the trans configuration. On the basis of chemical shift similarities with **3a** (Supporting Information), the isomer **3b** (7% of the total population) was tentatively



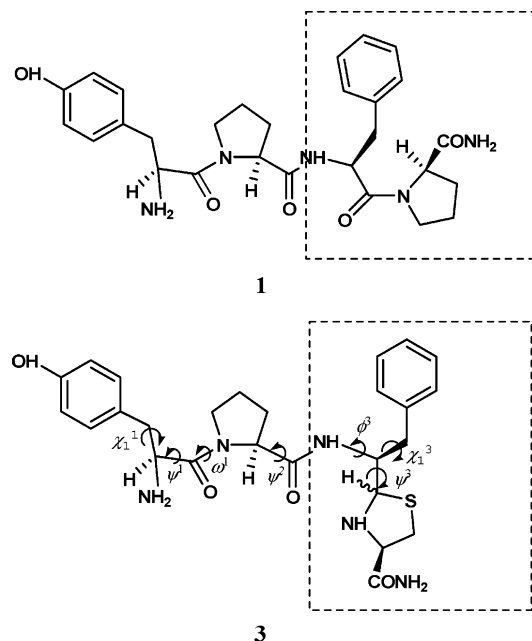


**Figure 3.** Structures of morphiceptin (**1**) and its active analogue **3**. Torsion angles given in the figure define spatial orientation of opioid pharmacophores. C-Terminal (*pseudo*) dipeptide has been indicated.

indicated as *trans*; therefore, the overall *Pro*<sup>2</sup> *trans* population of **3** raises to  $\approx 90\%$  of the total. Absolute configuration at C-2 of the thiazolidine ring of **3a** (Figure 1) was established on the basis of the observed NOEs. In fact, NOEs with different intensities were observed between the methylene protons ( $H_{C-5}$ ) of this ring and  $HC-4$  or  $HC-2$  ( $HC-5_{lf}/HC-4$ , strong;  $HC-5_{hf}/HC-4$ , medium;  $HC-5_{lf}/HC-2$ , not observed;  $HC-5_{hf}/HC-2$ , weak; where *hf* and *lf* mean high field and low field, respectively); furthermore, no NOE was observed between  $HC-4$  and  $HC-2$ . This NOE pattern is consistent with an anti orientation of  $HC-4$  and  $HC-2$  which defines the *S* configuration at C-2.

Analysis of short and medium-range NOEs,  $^3J_{NH-H\alpha}$  and  $^3J_{H\alpha-H\beta}$  coupling constants, HN exchange rates, and temperature coefficients for exchanging HN's was used to characterize main conformational features of **3a** (Table 3, and Supporting Information). Backbone conformation is defined by the angles showed in Figure 3. Since *Tyr*<sup>1</sup> is immediately followed by a proline, angle  $\psi^1$  rotation is highly restricted to a range of  $60^\circ$ – $180^\circ$ .<sup>14</sup> Strong sequential NOE from the  $H\alpha$  of *Pro*<sup>2</sup> to the HN of the *pseudo*-dipeptide indicates that the  $\psi^2$  angle is restricted to a range of  $60^\circ$ – $180^\circ$ . Small value of  $^3J_{NH-H\alpha}$  (4.5 Hz) and strong intraresidue NOE between the HN and the  $HC-1'$  of the *pseudo*-Phe<sup>3</sup> establishes a nearly *gauche* orientation of these two protons ( $\phi^3 \approx -60^\circ$ ). Coupling constant value between  $HC-1'$  and  $HC-2$  within the *pseudo*-dipeptide moiety ( $^3J = 9.7$  Hz) and medium intensity NOE between the same proton signals indicate a nearly *trans* orientation of these two atoms. Finally, slow exchange rate of amide proton of *pseudo*-Phe<sup>3</sup>, and a low value of the temperature coefficient for the same proton ( $-\Delta\delta/\Delta T < 3.0$  ppb/K), indicate that such proton is engaged in a hydrogen bond, probably stabilizing a turn structure. A turn structure is supported by the observation of weak NOE between  $H\alpha$  of *Tyr*<sup>1</sup> and HN of Phe<sup>3</sup>.

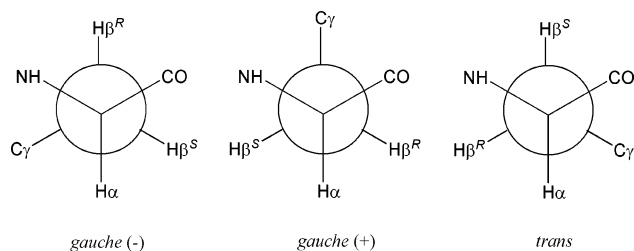


**Figure 4.** Newman projections about the  $C\alpha$ – $C\beta$  bond in the side chains of the *Tyr* and *Phe* residues. The two  $\beta$ -protons are distinguished by superscripts *R* and *S* (for *pro-R* and *pro-S* proton, respectively). For the *pseudo*-Phe<sup>3</sup> residue of **3** the symbol CO represents the thiazolidine carbon atom C-2.

Conformations around the  $C\alpha$ – $C\beta$  bond ( $\chi_1$ ) of the *Tyr*<sup>1</sup> and *pseudo*-Phe<sup>3</sup> residues are illustrated by the Newman projections in Figure 4, where the two  $\beta$ -protons are distinguished by superscripts *R* and *S* (for *pro-R* and *pro-S* proton, respectively). The *pro*chiralities of the  $\beta$ -protons of *Tyr*<sup>1</sup> and *pseudo*-Phe<sup>3</sup> were assigned by a combination of the observed  $^3J_{H\alpha-H\beta}$  values and NOEs including these  $\beta$ -protons. For the first residue, strong and medium NOEs were observed from the *Tyr*<sup>1</sup>  $H\alpha$  and *Pro*<sup>2</sup>  $H\delta$ 's to the *Tyr*<sup>1</sup>  $H\beta_{lf}$  which shows a small  $^3J_{H\alpha-H\beta}$  coupling constant (4.0 Hz) whereas weak NOEs were measured to *Tyr*<sup>1</sup>  $H\beta_{hf}$  showing a large  $^3J_{H\alpha-H\beta}$  value (10.8 Hz). As mentioned above, torsion angle  $\psi^1$  is restricted in a range from  $60^\circ$  to  $180^\circ$ . By use of molecular models with  $\psi^1$  in this region, the observed NOE between *Tyr*<sup>1</sup>  $H\beta_{lf}$  and *Pro*<sup>2</sup>  $H\delta$ 's allows us to identify the  $\beta$ -protons as follows:  $H\beta(R) = H\beta_{hf}$  and  $H\beta(S) = H\beta_{lf}$ . Fractions of the three side chains conformers  $\chi_1 = g^-, t, g^+$  of *Tyr*<sup>1</sup> were estimated by employing the rotational isomeric state approximation.<sup>29</sup> The *trans* ( $J_T$ ) and *gauche* ( $J_G$ ) coupling constants required for the analysis were set to 13.85 and 3.55 Hz following Cung et al.<sup>30</sup> The calculated  $\chi_1^1$  fractions ( $f(g^-) = 0.70$ ,  $f(t) = 0.04$ , and  $f(g^+) = 0.26$ ) indicate a large prevalence of the *g*<sup>−</sup> isomer. For the *pseudo*-Phe<sup>3</sup> residue intraresidue strong NOE was observed from the  $H\alpha$  ( $H\alpha$  stands for  $HC-1'$  and  $H\beta$  for  $HC-2'$ ) to the  $H\beta_{hf}$  which shows a small  $^3J_{H\alpha-H\beta}$  coupling constant (4.5 Hz) whereas medium NOE was measured to  $H\beta_{lf}$  showing a large  $^3J_{H\alpha-H\beta}$  value (10.5 Hz); medium intraresidue NOEs were observed from the HN to both  $H\beta$ 's; medium and weak sequential NOEs were observed from  $HC-2$  to  $H\beta_{lf}$  and  $H\beta_{hf}$ , respectively. Molecular model with *pseudo*  $\psi^3 \approx 180^\circ$  (see above) allows us to identify the  $\beta$ -protons as follows:  $H\beta(R) = H\beta_{hf}$  and  $H\beta(S) = H\beta_{lf}$ . The lacking of  $J_T$  and  $J_G$  reference values for this *pseudo*-Phe<sup>3</sup> residue prevented us from estimating the conformer fractions. Anyway, the whole pattern of described NOE points out to a *trans* conformation of the *pseudo*-Phe<sup>3</sup> side chain.

NMR-derived constraints for **3a** were used as the input data for a simulated annealing structure calculation as implemented within the standard protocol of the DYANA program.<sup>31</sup> The annealing procedure produced 200 conformations from which 50 structures were chosen, whose interprotonic distances best fitted NOE derived distances, and then refined through successive steps of restrained and unrestrained EM calculations using the program Discover (Biosym, San Diego, CA). For each peptide, 10 structures satisfying the NMR-derived constraints (violations smaller than 0.10 Å) were

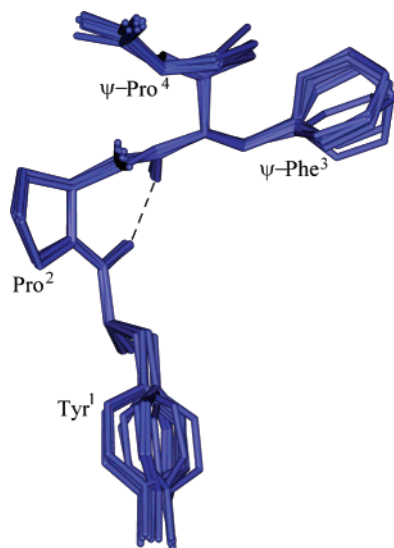


**Figure 5.** Superposition of the 10 lowest energy conformers of **3a**. Structures were superimposed using the backbone heavy atoms. Hydrogen atoms are not shown for clarity, except *pseudo*-Phe<sup>3</sup> HN, which is engaged in a hydrogen bond with the backbone carbonyl oxygen of Tyr<sup>1</sup> (broken line).

**Table 4.** Torsion Angles Defining the Pharmacophore Orientations of Described Compounds<sup>a</sup>

| angle      | <b>3a</b> <sup>b</sup> | <b>EM1</b> <sup>c</sup> | <b>1 all-trans</b> <sup>b</sup> | <b>1 cis-trans</b> <sup>b</sup> | <b>MC</b> <sup>c</sup> |
|------------|------------------------|-------------------------|---------------------------------|---------------------------------|------------------------|
| $\psi^1$   | 156 ± 6                | 150                     | 154 ± 6                         | 84 ± 10                         | 60–180                 |
| $\chi_1^1$ | g <sup>-</sup>         | g <sup>-</sup>          | g <sup>+</sup> , g <sup>-</sup> | t                               | t                      |
| $\omega^1$ | 176 ± 5                | 180                     | 175 ± 5                         | 0 ± 5                           | 0                      |
| $\psi^2$   | 91 ± 5                 | 150                     | 43 ± 8                          | 133 ± 5                         | 150                    |
| $\phi^3$   | -70 ± 8 <sup>d</sup>   | -120                    | -131 ± 11                       | -143 ± 9                        | -120                   |
| $\psi^3$   | 39 ± 4 <sup>d</sup>    | -30                     | 114 ± 11                        | 128 ± 5                         | 130                    |
| $\chi_1^3$ | t                      | t, g <sup>+</sup>       | t                               | t                               | t                      |

<sup>a</sup> Angles are in degrees. <sup>b</sup> Angles value of the mean structure of the 10 lowest energy conformers for **3a**, **1 all-trans**, and **1 cis-trans** are reported (± standard deviation). <sup>c</sup> **EM1**: Endomorphin-1 active structure from ref 9 (*trans*-endomorphin-1 'extended structure'). **MC**: Morphiceptin active structure from ref 14 (topology I). <sup>d</sup> *Pseudo*- $\phi^3$  and *pseudo*- $\psi^3$  angles.

chosen for further analysis. Structure **3a** was well defined, possessing average rms deviations of the backbone heavy atoms and of all heavy atoms equal to 0.20 and 0.45 Å, respectively (Figure 5, and Table 4). The analysis of the secondary structure showed the existence of an inverse  $\gamma$ -turn motif (C-7 turn) encompassing residues 1–3. This well-conserved region is stabilized by a hydrogen bond between *pseudo*-Phe<sup>3</sup> HN and Tyr<sup>1</sup> CO. The side chain of Tyr<sup>1</sup> and *pseudo*-Phe<sup>3</sup> are also well defined showing a preference for *g*- and *trans* orientations, respectively.

**Morphiceptin in SDS Micelles.** In the 1D <sup>1</sup>H NMR spectrum of **1** in SDS micelles, four distinct sets of signals are detected which arise from the *cis/trans* isomerization of the Tyr-Pro and Phe-Pro peptide bonds. Integration of the signals in the 1D spectrum reveals a ratio of 60:25:10:5. The major isomer has been assigned to the all-*trans* structure. The second largest isomer accounting for 25% adopts a *cis* configuration around the Tyr-Pro amide bond. Complete resonance assignment of the all-*trans* and of the *cis-trans* isomers was achieved (Table 3). Since only few signals unambiguously belong to the two minor isomers, assignment and structure determination were not possible in these cases, even though their configurations at Pro<sup>2</sup> and Pro<sup>4</sup>

were established through chemical shifts comparison with the major isomers (Supporting Information). All spectral parameters for both all-*trans* and *cis-trans* isomers are listed in Table 3 and the complete list of the NOE contacts are reported in the Supporting Information. Following similar arguments as those used for the isomer **3a** we could deduce the conformational preferences of both the all-*trans* and *cis-trans* isomers of **1**. Principal spectral features for the all-*trans* isomer were: the overlapping of the resonances of the Tyr<sup>1</sup> H $\beta$ 's which indicates side chain conformational averaging for this residue; the NOE contacts of H $\beta$ 's and H $\alpha$  of Tyr<sup>1</sup> with HN of Phe<sup>3</sup> which indicated the presence of a bent structure about the Pro<sup>2</sup> residue; the presence of some NOE contacts between the side chains of residues 1 and 3 which indicate their spatial proximity, again indicating the presence of a bent structure in the segment 1–3. The temperature coefficient ( $-\Delta\delta/\Delta T = 6.0$  ppb/K) of the amide protons of Phe<sup>3</sup> and its fast exchange rate in D<sub>2</sub>O/micelles solution indicate full accessibility of this proton to the solvent and the absence of a defined secondary structure.

In the *cis-trans* isomer, the *cis* configuration about the Pro<sup>2</sup> omega angle was evidenced by a sequential NOE connectivity between the H $\alpha$  atom signals of Tyr<sup>1</sup> and of Pro<sup>2</sup> while the NOE connectivities between the Phe<sup>3</sup> H $\alpha$  with the Pro<sup>4</sup> H $\delta$ 's established the *trans* configuration of the Pro<sup>4</sup> omega angle. For residues followed by a *cis* proline residues the  $\psi$  angle range is precluded to 60–180° as for those followed by *trans* prolines.<sup>14</sup> Therefore, the Tyr<sup>1</sup> and Phe<sup>3</sup> residues of morphiceptin adopt only the structures with  $\psi$  angles within this range. Two conformational states with ( $\phi, \psi$ )  $\approx$  (-75°, 135°) and ( $\phi, \psi$ )  $\approx$  (-75°, -40°) are probable for the *cis* configurational isomers of a proline embedded in a long peptide sequence.<sup>14</sup> Strong sequential NOE from the H $\alpha$  of Pro<sup>2</sup> to the HN of Phe<sup>3</sup> indicates an extended conformation at  $\psi^2$  ( $\psi^2 \approx 135^\circ$ ). NOE pattern indicates an extended conformation also for residue 3 ( $\phi, \psi$ )  $\approx$  (-140°, 120°). Finally, the preferred orientations of the side chains of the residues Tyr<sup>1</sup> and Phe<sup>3</sup> were assigned by a combination of the observed <sup>3</sup>J<sub>H $\alpha$ -H $\beta$  values and NOEs including their  $\beta$ -proton signals. As shown in Table 4, a preferred *trans* orientation of the side chains of both the aromatic residues is observed.</sub>

Structure calculation for all-*trans* and *cis-trans* isomers were performed as described for compound **3**. The 10 lowest energy and least violated conformers resulting from calculation are reported for both isomers in Figure 6, where the mean rms deviations from backbone superimposition are 0.40 Å and 0.30 Å for the all-*trans* and *cis-trans* isomers, respectively. Violations smaller than 0.15 Å were encountered for both the isomers. Regardless the well-defined structure of these isomers, no standard pattern of secondary structure could be observed. The side chain conformation is well defined for the *cis-trans* isomer (rms deviation from heavy atoms superimposition is 0.60 Å), which shows a *trans* orientation of both the Tyr and the Phe side chains. In the all-*trans* isomer the Tyr side chain is flexible and can adopt both the *g*- and the *g*<sup>+</sup> conformations while the Phe side chain is more defined showing a *trans* orientation. The conformational analysis indicates that the separation of the aromatic rings of the tyrosine and

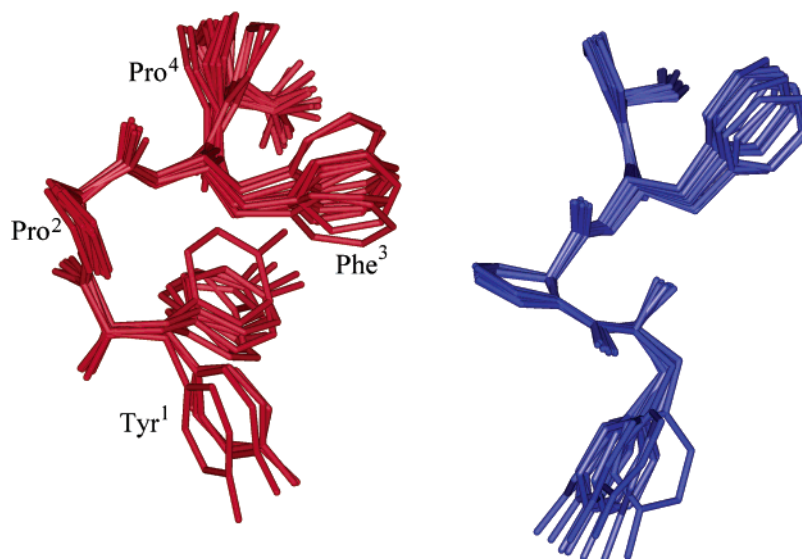


**Figure 6.** Superposition of the 10 lowest energy conformers of all-trans (red) and cis-trans (blue) isomers of **1**. Structures were superimposed using the backbone heavy atoms. Hydrogen atoms are not shown for clarity.

phenylalanine residues, as expressed by the center-to-center distance, is  $d_{\phi-\phi} = 10.5\text{--}11.0\text{ \AA}$  for the cis-trans isomer. For the all-trans isomer  $d_{\phi-\phi} \approx 5.0$  and  $d_{\phi-\phi} \approx 7.5\text{ \AA}$  are observed for conformers presenting the  $\chi_1^1$  angle in the  $g^+$  and  $g^-$  orientation, respectively.

## Discussion

Extensive structure-function studies on opioid receptor agonists and antagonists have been performed in attempts to understand the conformational requirements of these ligands for selective interaction with the different opioid receptors.<sup>3,4</sup> There is general consensus that the N-terminal portion of the opioid peptides acts as the message unit and that it contains three pharmacophoric groups: a positive ionizable feature placed on the amino terminal group of Tyr<sup>1</sup>; two hydrophobic aromatic features positioned onto the Tyr<sup>1</sup> aryl rings and a second aromatic residue in the third or fourth position. The two aromatic residues are separated by an appropriate spacer. In this context, the Tyr<sup>1</sup> residue plays the role of the primary pharmacophore while the orientation of the second aromatic pharmacophore relative to the tyrosine side chain dictates the receptor selectivity. In particular, a relatively large separation of the two aromatic side chains (10–13 Å) is required for the  $\mu$ -opioid receptor activity of these peptides.<sup>13</sup> In the  $\mu$ -selective opioid peptides morphiceptin and endomorphin-1 and -2 the spacer between the two pharmacophoric aromatic residues is represented by a proline residue. Furthermore, morphiceptin bears a second proline residue in the fourth position.

To gain information about the structural requirements of  $\mu$ -selective opioid peptides, we studied some morphiceptin derivatives introducing in this endogenous hormone a dipeptide mimetic structure that we have recently synthesized (Figure 1).<sup>19</sup> The rational basis of this substitution was the elimination of the amide bond in the dipeptide Xaa-Pro responsible of the cis-trans isomerization. In the dipeptide mimetic that we have developed this amide bond is absent, replaced by a single rotatable bond between the C-1' and the C-2 of the dipeptide mimetic structure.

Biological data (Figure 2, and Table 2) indicate that while the replacement of Tyr<sup>1</sup>-Pro<sup>2</sup> with the corresponding *pseudo*-dipeptide caused almost a complete loss of biological activity (compound **2**), replacement of residues 3–4 with an appropriate *pseudo*-dipeptide was tolerated at the  $\mu$ -opioid receptor. In fact, compound **3** showed similar activity to morphiceptin both in binding and functional assays, while compounds **4** and **5** were slightly less potent than the parent peptide in functional assays, even if they showed 12- and 7-fold reduced affinities, compared to morphiceptin in binding assay.

Hence, the amide bond at the Tyr<sup>1</sup>-Pro<sup>2</sup> appears to be indispensable for the biological activity of the morphiceptin, probably because the conformational restrictions imposed by the cis or trans configuration of this bond are necessary to the correct spatial disposition of the peptide.

Starting from the biological data, we have studied the conformational behavior of the most active analogue (**3**) and of the parent peptide morphiceptin (**1**) in the SDS membrane-like environment. The use of SDS micelles to study the conformational properties of these peptides is based on their interaction with a membrane receptor. For peptides acting as ligand of membrane receptors, the use of membrane mimetic media, such as SDS or dodecylphosphocoline, is suggested, hypothesizing a membrane-assisted mechanism of interactions between the peptides and their receptors.<sup>23</sup> Exploring the conformational behavior of peptide hormones in membrane-mimetic environment, we have recently succeeded in correlating receptor binding affinity of urotensin-II analogues with their preferred conformation in an SDS micelle solution.<sup>32</sup> Analogue **3** shows a trans configuration at Tyr<sup>1</sup>-Pro<sup>2</sup> amide bond (about 90% of the isomer populations) and a well-defined inverse  $\gamma$ -turn structure centered on Pro<sup>2</sup> residue (Figure 5). Side chains of the aromatic residues are also well defined with  $g^-$  and trans preferred orientation of the  $\chi_1$  angles of Tyr<sup>1</sup> and *pseudo*-Phe<sup>3</sup>, respectively.

As shown in Figure 7, the calculated structure of **3** can be efficiently superimposed to the 'active' structure of endomorphin-1 described by Podlogar et al.<sup>9</sup> This



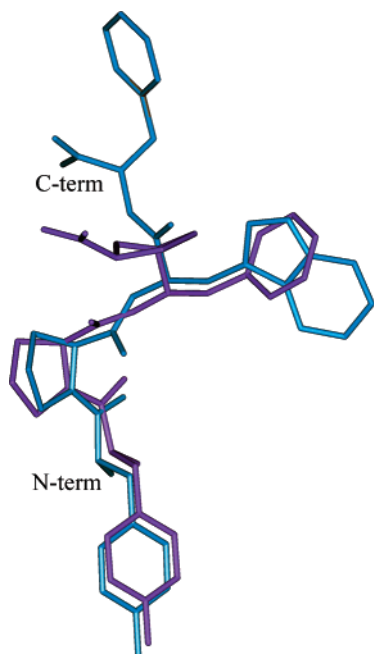


**Figure 7.** Superposition of the lowest energy structure of **3a** (violet) with that of endomorphin-1 (azure) described by Podlogar et al.<sup>9</sup> Structures were superimposed using the heavy atoms of residues 1–3. Hydrogen atoms are not shown for clarity.

structure, termed ‘trans-endomorphin-1 extended structure’, was derived by the authors from NMR analysis performed both in DMSO and in water followed by MD calculations. The authors found that endomorphin-1 exists in the cis and trans configuration with respect to the Tyr<sup>1</sup>-Pro<sup>2</sup> amide bond in approximately 25% and 75% populations, respectively. The trans structure was indicated as the bioactive one considering how it efficiently overlaid with other selective  $\mu$  ligands, PL-017 and D-TIPP. The hypothesis of a trans configuration of the Pro-omega bond for the bioactive conformation of endomorphin-1 was challenged by Fiori et al.<sup>11</sup> These authors, analyzing the conformational behavior of endomorphin-1 in AOT reverse micelles, proposed a different bioactive model for the peptide. In this model the configuration of the Pro-omega bond was cis and the two pharmacophoric aromatic residues were indicated as the first (Tyr<sup>1</sup>) and the fourth (Phe<sup>4</sup>). In contrast, Podlogar et al.<sup>9</sup> indicated the pharmacophoric aromatic residues as the first (Tyr<sup>1</sup>) and the third (Trp<sup>3</sup>) of the endomorphin-1. In this context, our compound **3** possesses unique structural features which avoid possible ambiguities. First, it shows an almost pure trans configuration at the Tyr<sup>1</sup>-Pro<sup>2</sup> amide bond, which is not the case for the other  $\mu$ -opioid selective peptide agonists containing the Tyr<sup>1</sup>-Pro<sup>2</sup> amide bond studied to date. Second, differently from endomorphin-1, compound **3** lacks the aromatic residue in position 4; therefore, the two aromatic pharmacophoric points are placed onto the aromatic rings of the first and of the third residues.

Interestingly, an inverse  $\gamma$ -turn structure has been recently proposed by Tóth and co-workers as the favored conformation of morphiceptin, endomorphin-1 and -2.<sup>33</sup> These authors analyzed the conformational behavior of these peptides by the simulated annealing method and solvated molecular dynamic calculations. It is worth to note that the N-terminal inverse  $\gamma$ -turns were found

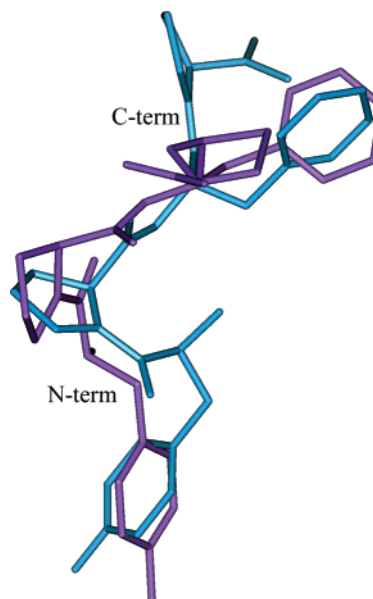


**Figure 8.** Superposition of the lowest energy structure of **3a** (violet) with that of the cis-trans isomer of **1** (azure). Structures were superimposed using the side chain heavy atoms of residues 1–3. Hydrogen atoms are not shown for clarity.

only in the Pro<sup>2</sup> trans conformers: they were absent from the cis conformers.

Regarding the micelle-bound structures of the morphiceptin, two major isomers could be observed with the all-trans or the cis-trans configurations at the two X-Pro amide bonds (Figure 6). The largest differences between the isomers are observed for the relative spatial arrangement of the two aromatic side chains of the Tyr and the Phe residues. The all-trans isomer assumes a rather compact structure with small distances,  $d_{\phi-\phi} = 5.0\text{--}7.5\text{ \AA}$ , between the two aromatic rings of the Tyr and Phe residues. On the other hand, relatively large values of distance ( $d_{\phi-\phi} = 10.5\text{--}11.0\text{ \AA}$ ) are observed for the minimum energy conformations estimated for the cis-trans isomer. The results obtained from the conformational analysis leads to the conclusion that only the cis-trans isomer displays the relative large separation of Tyr<sup>1</sup> and Phe<sup>3</sup> side chains which is required for the  $\mu$ -opioid receptor activity.<sup>13</sup> Interestingly, the structural parameters corresponding to the cis-trans isomer, that we have found, are highly consistent with the topochemical model proposed by Yamazaki et al.<sup>14</sup> for the morphiceptin bioactive conformation (see Table 4). In fact, this model consists of a cis configuration of Tyr<sup>1</sup>-Pro<sup>2</sup> amide bond and a trans orientation of the Tyr<sup>1</sup> as well as of the Phe<sup>3</sup> side chains.

The results obtained for compound **3** and for morphiceptin seem to be in contrast since a trans configuration of Tyr<sup>1</sup>-Pro<sup>2</sup> amide bond has been found for the ‘active’ structure of the first while a cis configuration at this bond is required for the latter. To gain insight into this apparent contradiction, we superimposed the obtained micelles bound structure of **3** with that of the parent morphiceptin. As shown in Figure 8, despite the different configuration at Pro<sup>2</sup> amide bond, the two structures display similar topological arrangement. In particular, the pharmacophoric distance from Tyr center to the center of the Phe aromatic ring is very similar in the two analogues, both in the range of 10–11 Å, a result



in accordance with the  $\mu$ -opioid receptor requirement.<sup>13</sup> Also, the corresponding aromatic moieties of the two compounds have similar spatial orientations. This finding agrees with the assumption that the location and the relative orientation of the aromatic side chains, rather than a peculiar backbone conformation, dictate the selectivity toward the  $\mu$ -opioid receptor and that the principal role of the other residues is confined to the stabilization of one specific bioactive conformation among the pool of structures accessible for such short, conformational unrestrained peptides.<sup>34</sup>

N-Terminal tyrosine residue is a common structural feature of opioid peptides. Actually, the hydroxy phenyl ring and the positively charged nitrogen are a general requirement for nearly all of the reported opioid ligand pharmacophores.<sup>35</sup> The relative disposition of these pharmacophoric points is fully defined by  $\chi_1$  angle of Tyr<sup>1</sup>. We found different  $\chi_1$  angle values of Tyr<sup>1</sup> for compound **3** ( $\chi_1 \approx 60^\circ$ ) and morphiceptin ( $\chi_1 \approx 180^\circ$ ). This difference would indicate that the  $\mu$ -opioid receptor can accommodate both the *g*- and *trans* tyrosine side chain conformations, again indicating a high degree of structural tolerance within the receptor binding site.

Finally, it is interesting to note the dramatic influence of the C-terminal residue on the overall conformational behavior of the peptides that we investigated. This influence could explain some results previously reported in the literature. For instance, the inactivity of the 'all *trans*' 2-methyl proline derivative of the morphiceptin<sup>36</sup> and of other *trans* constrained *pseudo*-Pro<sup>2</sup> derivatives<sup>16</sup> can be explained, admitting that the morphiceptin analogues with a proline residue at position 4 cannot reach the appropriate active conformation when they adopt the *trans* configuration at Pro<sup>2</sup> omega bond. In contrast, above data suggest that the presence of other C-terminal residues, such as phenylalanine in the endomorphins and our *pseudoproline* in compound **3**, allows the existence of a compatible bioactive conformation also (or only) with the *trans* Pro<sup>2</sup> configuration. Eventually, the influence of the C-terminal residue on the overall conformation of the opioid peptides are in accordance with the biological result indicating that the potency of opioid tetrapeptides containing the Tyr-Pro-Phe-X-NH<sub>2</sub> or Tyr-Pro-Trp-X-NH<sub>2</sub> sequence is determined by the nature of the fourth residue.<sup>37</sup>

## Conclusions

In conclusion, comparing the biological and conformational behavior of some morphiceptin analogues with the parent peptide, we confirm a high degree of structural tolerance within the  $\mu$ -opioid receptor binding site. In fact, our results agree with the assumption that only the location and the relative orientation of the side chains of the aromatic pharmacophoric residues represent the indispensable structural feature for  $\mu$ -receptor binding. To reach such topological arrangement, the peptide can adopt different conformations and configurations. In particular, opioid peptides bearing a proline residue as spacer between the two aromatic residues can adopt, in active state, both *cis* and *trans* configurations at the Tyr<sup>1</sup>-Pro<sup>2</sup> amide bond, each of them with the appropriate backbone and side chain orientations. Our results also point to the importance of the C-terminal residue in dictating the overall conformational

preferences of these peptides. These data shed light on the topological requirements of the  $\mu$ -opioid receptor and therefore might be useful for the design of new ligands at this receptor of great pharmacological interest.

## Experimental Section

**Materials.** *N*<sup>α</sup>-Fmoc-protected amino acids, HBTU, HOBt, and Ring amide resin were purchased from Advanced Chem-Tech (Louisville, KY). Peptide synthesis solvents, reagents, as well as CH<sub>3</sub>CN for HPLC were reagent grade and were acquired from commercial sources and used without further purification unless otherwise noted. FAB-MS analyses were performed by MALDI. The purity of the finished peptides was checked by analytical RP-HPLC using a Shimadzu model CL-10AD VP system with a built-in diode array detector. In all cases, the purity of the finished peptides was greater than 95% as determined by these methods.

[<sup>3</sup>H]DAMGO (50 Ci/mmol) and [<sup>3</sup>H]naltrindole (35 Ci/mmol) were purchased from PerkinElmer Life and Analytical Science. Leupeptin, bacitracin, phenylmethanesulfonyl fluoride (PMSF), bestatin and DAMGO were products of Sigma-Aldrich Co. 7-Benzylidenenaltrexone (BNTX) was purchased from Tocris Cookson (Bristol, UK). Naloxone and loperamide were products of Alexis Corp. Morphine was purchased from Salars. Other agents and reagents were from standard commercial sources.

For NMR analysis, <sup>2</sup>H<sub>2</sub>O were obtained from Aldrich (Milwaukee, WI), 98% SDS-*d*<sub>25</sub> was obtained from Cambridge Isotope Laboratories, Inc. (Andover, MA), [(2,2,3,3-tetra-deuterio-3-(trimethylsilyl)l)propionic acid (TSP) from MSD Isotopes (Montreal, Canada).

**General Method for Peptide Synthesis and Purification.** All peptides were synthesized by the solid-phase method of peptide synthesis and purified by RP-HPLC. The peptides were synthesized on 0.15 g each of Rink amide resin (substitution 0.7 mmol/g) by manual methods using *N*<sup>α</sup>-Fmoc chemistry and an orthogonal side chain protection strategy. The entire synthesis was performed under argon. The resin was first swollen in DCM/DMF (1:1) for 2 h, and the following amino acids or the *pseudo*-dipeptide were then added to the growing peptide chain by stepwise addition of *N*<sup>α</sup>-Fmoc amino acids using standard solid-phase methods. Each coupling reaction was achieved using a 3-fold excess of each of the amino acid, HBTU, and HOBt in the presence of a 6-fold excess of DIPEA for 1 h. Deprotection of the *N*<sup>α</sup>-Fmoc group was carried out by treating the protected peptide resin with 25% piperidine solution in DMF (1 × 4 mL, 20 min). After each coupling and deprotection, the peptide resin was washed with DMF (3 × 4 mL), DCM (3 × 50 mL) and again with DMF. The peptide sequences were thus assembled by alternate cycles of coupling and deprotection. After coupling of the *N*-terminal amino acid, the *N*-terminal Fmoc group was deblocked as described above, and the peptide-resin was thoroughly washed with DCM (4 × 25 mL) and dried under argon to yield dried peptide-resin.

The peptide-resin was then cleaved by treating with 4 mL of a solution of Et<sub>3</sub>SiH (5%), water (5%), and *p*-thiocresol/*p*-cresol (0.1%, 1:1) in TFA with shaking at room temperature for 3 h. The resin was then removed from the solution by filtration, and the crude peptide was recovered by precipitation with cold anhydrous ethyl ether. Centrifugation at 1500g for 3 min followed by decantation of the supernatant ether and air-drying of the residue yielded the crude peptide as a white to pale beige colored amorphous solid.

Final peptide purification was achieved using a preparative RP-HPLC Vydac C18 (218TP1520, 15  $\mu$ m). The peptide samples were injected onto the column at a concentration of 20–30 mg/mL in 20% aqueous CH<sub>3</sub>CN and were eluted with a CH<sub>3</sub>CN gradient (10 to 90%) over 40 min at a flow rate of 15.0 mL/min, with a constant concentration of TFA (0.1% v/v). The separations were monitored at 230 and 280 nm and integrated with a Shimadzu diode array detector mod. SPD-M10A VP dual wavelength absorbance detector model UV-D. Fractions corresponding to the major peak were collected, pooled, and lyophilized to yield the final peptides as pure

**Table 5.** Inhibition of [<sup>3</sup>H]Naltrindole Binding to Brain Membranes by Morphiceptin Analogues

| compound (10 $\mu$ M) | % of inhibition (mean $\pm$ SEM) <sup>a</sup> |
|-----------------------|---|
| <b>1</b>              | 23.6 $\pm$ 4 ( <i>n</i> = 4)                  |
| <b>2</b>              | 10.2 $\pm$ 4 ( <i>n</i> = 3)                  |
| <b>3</b>              | 22.7 $\pm$ 8 ( <i>n</i> = 3)                  |
| <b>4</b>              | 42.2 $\pm$ 12 ( <i>n</i> = 3)                 |
| <b>5</b>              | 67.8 $\pm$ 14 ( <i>n</i> = 3)                 |

<sup>a</sup> *n*: number of experiments.

(>95%) white solids. The analytical data for each compound are presented in Table 1.

**Binding Assay.** The preparation of whole brain (minus cerebellum) membranes for opioid  $\delta$  and  $\mu$  receptor binding experiments was carried as described previously.<sup>38</sup> Protein concentration was determined by the method of Lowry et al.<sup>39</sup> using bovine serum albumin (BSA) as standard.

For labeling opioid  $\mu$  receptors, brain membranes (0.3 mg of protein) were incubated with 0.7–1 nM [<sup>3</sup>H]DAMGO in 1 mL of 50 mM Tris-HCl, pH 7.4, 5 mM MgCl<sub>2</sub> (buffer A) containing 10  $\mu$ g/mL bacitracin, 2  $\mu$ g/mL bestatin, 5  $\mu$ g/mL leupeptin, 4  $\mu$ g/mL trypsin inhibitor, and 0.1 mM phenylmethanesulfonyl fluoride (PMSF) at 25 °C for 2 h. Nonspecific binding was measured in the presence of 10  $\mu$ M 7-benzylidenenaltrexone (BNTX). Incubation was terminated by filtration through GF/C filters (Millipore) previously treated with 0.3% polyethyleneimine for more than 1 h. Then filters were washed three times with 5 mL of ice-cold buffer A, and radioactivity was measured using a liquid scintillation cocktail by a Packard TRI-CARB 1600 scintillation counter (Packard Instrument, Meriden, CT). For labeling opioid  $\delta$  receptors, binding studies were performed as described by Santagada et al.<sup>38</sup> using [<sup>3</sup>H]naltrindole as radioligand. Compound concentrations of 1 to 10  $\mu$ M produced modest reductions of [<sup>3</sup>H]naltrindole binding to membranes but caused a consistent inhibition of [<sup>3</sup>H]DAMGO binding. In Table 5, the inhibitory effects of 10  $\mu$ M morphiceptin analogues on [<sup>3</sup>H]naltrindole binding are shown. Competition studies were carried out by incubating membranes in buffer A with 0.7 nM [<sup>3</sup>H]DAMGO and 11 newly synthesized peptides (1 nM to 10  $\mu$ M).

**Functional Assay.** The pharmacological procedures were carried out following the guidelines of the European Council Directive 86/609 concerning animal experimentation. For the functional study, compounds were tested on electrostimulated ileum of male Dunkin Hartley guinea pigs (300–350 g). The animals were sacrificed by cervical dislocation and bled, under light ether anaesthesia. Segments of ileum (2–3 cm in length) were excised (5–6 cm far from the ileo-cecal valve), freed of extraneous tissues, and suspended between two platinum electrodes, under a preload of 0.5 g, in 10 mL organ baths, containing Tyrode saline (composition in mM: 136.80 NaCl, 2.95 KCl, 1.80 CaCl<sub>2</sub>, 1.05 MgSO<sub>4</sub>·7H<sub>2</sub>O, 0.41 NaH<sub>2</sub>PO<sub>4</sub>, 11.90 NaHCO<sub>3</sub>, 5.50 glucose), thermostated at 37 °C, and continuously bubbled with a mixture of O<sub>2</sub> (95%) and CO<sub>2</sub> (5%).

After 30–40 min of equilibration time, the electrical field stimulation (EFS) started (train duration 100 ms; pulse width 1 ms; pulse interval 10 ms; supramaximal voltage 20 V). When the electrically induced contractile spikes reached a stable control width, 3-fold increasing concentrations (0.1 nM to 1  $\mu$ M) of the tested compounds and reference opioid agonists, morphine, DAMGO and loperamide, were added cumulatively. In parallel sets of experiments, compounds were added in the presence of the opioid antagonist naloxone (10 nM). Changes in isotonic tension were recorded by isotonic transducers (Basile mod. 7006) connected to microdynamometers (Basile mod. 7050).

**Biological Data Analysis. 1. Binding Assay.** Data were analyzed by a nonlinear least-squares fitting, using the GraphPad Prism Version 3.00 computer program. Single- and multiple-site models were statistically compared to determine the best fit, and differences between models were tested by comparing the residual variance using a partial F test and a significance level of *P* < 0.05 (GraphPad Prism Version 3.00). The IC<sub>50</sub> values obtained from displacement and dilution

curves were converted to *K<sub>i</sub>* values by the Cheng and Prusoff equation<sup>40</sup> using the value of 1.3 nM as dissociation constant (*K<sub>D</sub>*) for [<sup>3</sup>H]DAMGO. Values represent the mean  $\pm$  SEM of at least three independent experiments.

**2. Functional Assay.** The inhibitory effects of test compounds and of reference agonists were evaluated as percentage of the control width (0 = no effects; 100 = full abolition of the EFS-induced contractile spikes). The parameter of agonist efficacy reflected the maximal inhibitory effect recorded, while the potency parameter was expressed as EC<sub>50</sub>, representing the concentration evoking a half-maximal inhibitory effect. Data, expressed as mean  $\pm$  SEM for 4–6 experiments, were statistically analyzed by Student *t* test and Anova. *P* values lower than 0.05 were considered as representative of statistical significance.

**NMR Spectroscopy.** The samples for NMR spectroscopy were prepared by dissolving the appropriate amount of peptide in 0.45 mL of <sup>1</sup>H<sub>2</sub>O (pH 5.5), 0.05 mL of <sup>2</sup>H<sub>2</sub>O to obtain a concentration 1–2 mM of peptides, and 200 mM of SDS-*d*<sub>25</sub>. NH exchange studies were performed dissolving peptides in 0.50 mL of <sup>2</sup>H<sub>2</sub>O and 200 mM of SDS-*d*<sub>25</sub>. NMR spectra were recorded on a VARIAN Unity Inova 500 spectrometer. All the spectra were recorded at a temperature of 300 K. One-dimensional (1D) NMR spectra were recorded in the Fourier mode with quadrature detection, and the water signal was suppressed by a low-power selective irradiation in the homogenized mode. 2D DQF-COSY,<sup>25</sup> TOCSY,<sup>26</sup> and NOESY<sup>27</sup> experiments were run in the phase-sensitive mode using quadrature detection in  $\omega_1$  by time-proportional phase increase of initial pulse. Data block sizes were 2048 addresses in *t*<sub>2</sub> and 512 equidistant *t*<sub>1</sub> values. Before Fourier transformation, the time domain data matrixes were multiplied by shifted sin<sup>2</sup> functions in both dimensions. A mixing time of 70 ms was used for the TOCSY experiments. NOESY experiments were run at 300 K with mixing times in the range of 150–300 ms. The spectra were calibrated relative to TSP (0.00 ppm) as internal standard. The qualitative and quantitative analyses of DQF-COSY, TOCSY, and NOESY spectra, were obtained using the interactive program package XEASY.<sup>28</sup> <sup>3</sup>*J*<sub>HN-H $\alpha$</sub>  and <sup>3</sup>*J*<sub>H $\alpha$ -H $\beta$</sub>  coupling constants were obtained by 1D spectra and by sections of cross-peaks from the resolution enhanced 4K  $\times$  2K DQF-COSY spectra. The temperature coefficients of the amide proton chemical shifts were calculated from 1D <sup>1</sup>H NMR and 2D DQF-COSY experiments performed at different temperatures in the range 300–320 K by means of linear regression.

In the NOESY spectra of both morphiceptin and peptide **3**, all the cross-peaks show the same sign of the diagonal peaks, showing that the peptide interaction with the SDS micelles is taking place and that the whole system is moving in solution with  $\omega\tau_c \gg 1$ .

**Structural Determinations and Computational Modeling.** The NOE-based distance restraints were obtained from NOESY spectra collected with a mixing time of 200 ms. The NOE cross-peaks were integrated with the XEASY program and were converted into upper distance bounds using the CALIBA program incorporated into the program package DYANA.<sup>31</sup> Cross-peaks which were overlapped more than 50% were treated as weak restraints in the DYANA calculation. Nonstandard dipeptide mimetic moiety was added to DYANA residue library using MOLMOL.<sup>41</sup> Only NOE-derived constraints (Supporting Information) were considered in the annealing procedures. For each examined peptide, an ensemble of 200 structures was generated with the simulated annealing standard protocol of the program DYANA. 50/200 structures were chosen, whose interprotonic distances best fitted NOE derived distances, and then refined through successive steps of restrained and unrestrained EM calculations. First, steepest descents minimizations with distance restraints were performed on all structures with the Discover algorithm (Biosym, San Diego) utilizing the consistent valence force field (CVFF).<sup>42</sup> A generic distance maximum force constant of 100 kcal/mol and an upper distance force constants of 32 kcal/Å<sup>2</sup> were used. Minimization proceeded until the change in energy was less



than 0.05 kcal/mol. This was followed by 3000 steps of unrestrained steepest descents energy minimization. A distance-dependent dielectric constant equal to 4 $\epsilon$  was applied to evaluate electrostatic interactions. The minimization lowered the total energy of the structures; no residue was found in the disallowed region of the Ramachandran plot. The final structures were analyzed using the InsightII program (Biosym, San Diego, CA). Graphical representation were carried out with the InsightII program (Biosym, San Diego, CA). RMS deviation analysis between energy minimized structures were carried out with the program MOLMOL.<sup>41</sup> The PROMOTIF program was used to extract details on the location and types of structural secondary motifs.<sup>43</sup>

**Acknowledgment.** Authors thank Paolo Rovero (University of Florence, Italy) for helpful discussions. Authors also thank David M. Ferguson and Germana Paterlini (University of Minnesota) who kindly supplied the atomic coordinates of the endomorphin-1 calculated structure.

## Appendix

Abbreviations used for amino acids and designation of peptides follow the rules of the IUPAC–IUB Commission of Biochemical Nomenclature in *J. Biol. Chem.* **1972**, 247, 977–983. Amino acid symbols denote L-configuration unless indicated otherwise. The following additional abbreviations are used: AAA, amino acid analysis; AOT, bis(2-ethylhexyl)sulfosuccinate sodium salt; Boc, *tert*-butoxycarbonyl; Bzl, benzyl; *t*Bu, *tert*-butyl; CH<sub>3</sub>CN, acetonitrile; DCM, dichloromethane; DIPEA, *N,N*-diisopropylethylamine; DMF, *N,N*-dimethylformamide; DQF–COSY, double quantum filtered correlated spectroscopy; Et<sub>3</sub>SiH, triethylsilane; FAB-MS, fast-atom bombardment mass spectrometry; Fmoc, 9-fluorenylmethoxycarbonyl; HOBt, *N*-hydroxybenzotriazole; HBTU, 2-(1*H*-benzotriazole-1-yl)-1,1,3,3-tetramethyluronium hexafluorophosphate; MALDI-TOF, matrix-assisted laser desorption/ionization/time-of-flight mass spectrometry; MD, molecular dynamic; NMP, *N*-methyl pyrrolidinone; NMR, nuclear magnetic resonance; NOE, nuclear Overhauser effect; NOESY, nuclear Overhauser enhancement spectroscopy; RP-HPLC, reversed-phase high performance liquid chromatography; SDS, sodium dodecylsulfate; SPPS, solid-phase peptide synthesis; SPS, solid-phase synthesis; TFA, trifluoroacetic acid; TLC, thin-layer chromatography; TOCSY, total correlated spectroscopy; Trt, triphenylmethyl (trityl); TSP, 3-(trimethylsilyl)propionic acid.

**Supporting Information Available:** <sup>1</sup>H NMR assignments of the minor isomers of compounds **1** and **3**. Lists of NOE used in the structure calculations. This material is available free of charge via the Internet at <http://pubs.acs.org>.

## References

- Lord, J. A. H.; Waterfield, A. A.; Hughes, J.; Kosterlitz, H. W. Endogenous Opioid Peptides: Multiple Agonists and Receptors. *Nature* **1977**, 267, 495–499.
- Kieffer, B. L. Recent Advances in Molecular Recognition and Signal Transduction of Active Peptides: Receptors for Opioid Peptides. *Cell. Mol. Neurobiol.* **1995**, 15, 615–635.
- (a) Hruby, V. J.; Agnes, R. S. Conformation-Activity Relationships of Opioid Peptides with Selective Activities at Opioid Receptors. *Biopolymers* **1999**, 51, 391–410. (b) Hruby, V. J.; Balse, P. M. Conformational and Topographical Considerations in Designing Agonist Peptidomimetics from Peptide Leads. *Curr. Med. Chem.* **2000**, 7, 945–970.
- (a) Portoghese, P. S. The role of Concepts in Structure Activity Relationship Studies of Opioid Ligands. *J. Med. Chem.* **1992**, 35, 1927–1937. (b) Portoghese, P. S. From Models to Molecules: Opioid Receptor Dimers, Bivalent Ligands, and Selective Opioid Receptor Probes. *J. Med. Chem.* **2001**, 44, 2259–2269.
- Matthes, H. W.; Maldonado, R.; Simonin, F.; Valverde, O.; Slowe, S.; Kitchen, I.; Befort, K.; Dierich, A.; Le Meur, M.; Dolle, P.; Tzavara, E.; Hanoune, J.; Roques, B. P.; Kieffer, B. L. Loss of Morphine-Induced Analgesia, Reward Effect and Withdrawal Symptoms in Mice Lacking the  $\mu$ -Opioid-Receptor Gene. *Nature* **1996**, 383, 819–23.
- Chang, K. J.; Killian, A.; Hazum, E.; Cuatrecasas, P.; Chang, J. K. Morphiceptin (H-Tyr-Pro-Phe-Pro-NH<sub>2</sub>): a Potent and Specific Agonist for Morphine ( $\mu$ ) Receptors. *Science* **1981**, 212, 75–77.
- Zadina, J. E.; Hackler, L.; Ge, L. J.; Kastin, A. J. A Potent and Selective Endogenous Agonist for the  $\mu$ -Opiate Receptor. *Nature* **1997**, 386, 499–502.
- Goodman, M.; Mierke, D. Configurations of Morphiceptins by <sup>1</sup>H and <sup>13</sup>C NMR Spectroscopy. *J. Am. Chem. Soc.* **1989**, 111, 3489–3496.
- Podlogar, B. L.; Paterlini, M. G.; Ferguson, D. M.; Leo, G. C.; Demeter, D. A.; Brown, F. K.; Reitz, A. B. Conformational Analysis of the Endogenous  $\mu$ -Opioid Agonist Endomorphin-1 Using NMR Spectroscopy and Molecular Modeling. *FEBS Lett.* **1998**, 439, 13–20.
- In, Y.; Minoura, K.; Ohishi, H.; Minakata, H.; Kamigau, M.; Sugiura, M.; Ishida, T. Conformational Comparison of  $\mu$ -Selective Endomorphin-2 with its C-Terminal Free Acid in DMSO Solution, by <sup>1</sup>H NMR Spectroscopy and Molecular Modeling Calculation. *J. Pept. Res.* **2001**, 58, 399–412.
- Fiori, S.; Renner, C.; Cramer, J.; Pegoraro, S.; Moroder, L. Preferred Conformation of Endomorphin-1 in Aqueous and Membrane-Mimetic Environments. *J. Mol. Biol.* **1999**, 291, 163–175.
- Schwyzler, R. ACTH: A Short Introductory Review. *Ann. N. Y. Acad. Sci.* **1977**, 297, 3–26.
- Yamazaki, T.; Pröbstl, A.; Schiller, P. W.; Goodman, M. Biological and Conformational Studies of [Val<sup>4</sup>]Morphiceptin and [D-Val<sup>4</sup>]Morphiceptin Analogs Incorporating Cis-2-Aminocyclopentane Carboxylic Acid as a Peptidomimetic for Proline. *Int. J. Pept. Prot. Res.* **1991**, 37, 364–381.
- Yamazaki, T.; Ro, S.; Goodman, M.; Chung, N. N.; Schiller, P. W. A Topochemical Approach to Explain Morphiceptin Bioactivity. *J. Med. Chem.* **1993**, 36, 708–719.
- Paterlini, M. G.; Avitabile, F.; Ostrowski, B. G.; Ferguson, D. M.; Portoghese, P. S. Stereochemical Requirements for Receptor Recognition of the  $\mu$ -Opioid Peptide Endomorphin-1. *Biophys. J.* **2000**, 78, 590–599.
- Keller, M.; Boissard, C.; Patiny, L.; Chung, N. N.; Lemieux, C.; Mutter, M.; Schiller, P. W. Pseudoproline-Containing Analogues of Morphiceptin and Endomorphin-2: Evidence for a Cis Tyr-Pro Amide Bound in the Bioactive Conformation. *J. Med. Chem.* **2001**, 44, 3896–3903.
- Doi, M.; Asano, A.; Komura, E.; Ueda, Y. The Structure of an Endomorphin Analogue Incorporating 1-Aminocyclohexane-1-Carboxylic Acid for Proline is Similar to the  $\beta$ -turn of Leu-Enkephalin. *Biochem. Biophys. Res. Commun.* **2002**, 297, 138–142.
- Okada, Y.; Fujita, Y.; Motoyama, T.; Tsuda, Y.; Toshio, Y.; Li, T.; Sasaki, Y.; Ambo, A.; Jinsmaa, Y.; Bryant, S. D.; Lazarus, L. H. Structural Studies of [2',6'-Dimethyl-L-tyrosine<sup>1</sup>]Endomorphin-2 Analogues: Enhanced Activity and Cis Orientation of the Dmt-Pro Amide Bond. *Bioorg. Med. Chem.* **2003**, 11, 1983–1994.
- Grieco, P.; Campiglia, P.; Gomez-Monterrey, I.; Novellino, E. Synthesis of Conformationally Constrained  $\beta$ -turn Thiazolidine Mimetic. *Tetrahedron Lett.* **2002**, 43, 1197–1199.
- Stewart, J. M.; Young, J. D. In *Solid-Phase Peptide Synthesis*; Pierce Chemical: Rockford, IL, 1984.
- Fichna, J.; Do-Rego, J. C.; Costentin, J.; Chung, N. N.; Schiller, P. W.; Kosson, P.; Janecka, A. Opioid Receptor Binding and in Vivo Antinociceptive Activity of Position 3-Substituted Morphiceptin Analogs. *Biochem. Biophys. Res. Commun.* **2004**, 320, 531–536.
- Mosberg, H. I.; Hurst, R.; Hruby, V. J.; Galligan, J. J.; Burks, T. F.; Gee, K.; Yamamura, K. I. [D-Pen2, L-Cys5]Enkephalinamide and [D-Pen2, D-Cys5]Enkephalinamide, Conformationally Constrained Cyclic Enkephalinamide Analogs with  $\delta$  Receptor Specificity. *Biochem. Biophys. Res. Commun.* **1982**, 106, 506–512.
- Moroder, L.; Romano, R.; Guba, W.; Mierke, D. F.; Kessler, H.; Delporte, C.; Winand, J.; Christophe, J. New Evidence for a Membrane Bound Pathway in Hormone Receptor Binding. *Biochemistry* **1993**, 32, 13551–13559.
- Wüthrich, K. *NMR of Proteins and nucleic acids*; John Wiley & Sons: New York, 1986.

- (25) (a) Piantini, U.; Sorensen, O. W.; Ernst, R. R. Multiple Quantum Filters for Elucidating NMR Coupling Network. *J. Am. Chem. Soc.* **1982**, *104*, 6800–6801. (b) Marion, D.; Wüthrich, K. Application of Phase Sensitive Two-Dimensional Correlated Spectroscopy (COSY) for Measurements of  $^1\text{H}$ - $^1\text{H}$  Spin-Spin Coupling Constants in Proteins. *Biochem. Biophys. Res. Commun.* **1983**, *113*, 967–974.
- (26) Bax, A.; Davis, D. G. Mlev-17-Based Two-Dimensional Homonuclear Magnetization Transfer Spectroscopy. *J. Magn. Reson.* **1985**, *65*, 355–360.
- (27) Jenner, J.; Meyer, B. H.; Bachman, P.; Ernst, R. R. Investigation of Exchange Processes by Two-Dimensional NMR Spectroscopy. *J. Chem. Phys.* **1979**, *71*, 4546–4553.
- (28) Bartels, C.; Xia, T.; Billeter, M.; Guentert, P.; Wüthrich, K. The Program XEASY for Computer-Supported NMR Spectral Analysis of Biological Macromolecules. *J. Biomol. NMR* **1995**, *6*, 1–10.
- (29) Pachler, K. G. R. Nuclear Magnetic Resonance Study of Some  $\alpha$ -Amino Acids-II. Rotational Isomerism. *Spectrochim. Acta* **1964**, *20*, 581–587.
- (30) Cung, M. T.; Marraud, M. Conformational Dependence of the Vicinal Proton Coupling Constant for the  $\text{C}\alpha$ - $\text{C}\beta$  Bond in Peptides. *Biopolymers* **1982**, *21*, 953–967.
- (31) Guntert, P.; Mumenthaler, C.; Wüthrich, K.; Torsion Angle Dynamics for NMR Structure Calculation With the New Program DYANA. *J. Mol. Biol.* **1997**, *273*, 283–298.
- (32) Carotenuto, A.; Grieco, P.; Campiglia, P.; Novellino, E.; Rovero, P. Unraveling the Active Conformation of Urotensin II. *J. Med. Chem.* **2004**, *47*, 1652–1661.
- (33) Ötvös, F.; Körtvélyesi, T.; Tóth, G. Structure Activity Relationship of Endomorphin-1, Endomorphin-2 and Morphiceptin by Molecular Dynamics Methods. *J. Mol. Struct. (THEOCHEM)* **2003**, *666–667*, 345–353.
- (34) (a) Aubry, A.; Birlirakis, N.; Sakarellos-Daitsiotis, M.; Sakarellos, C.; Marraud, M. A Crystal Molecular Conformation of Leucine-Enkephaline Related to Morphine Molecule. *Biopolymers* **1989**, *28*, 27–40. (b) Gentilucci, L.; Tolomelli, A. Recent advances in the investigation of the bioactive conformation of peptide active at the  $\mu$ -opioid receptor. Conformational analysis of Endomorphins. *Curr. Top. Med. Chem.* **2004**, *4*, 105–121.
- (35) Huang, G.; Loew, G. Development of a Common 3D Pharmacophore for Delta-opioid Recognition from Peptides and Non-Peptides Using a Novel Computer Program. *J. Comput.-Aided Mol. Des.* **1997**, *11*, 21–28.
- (36) Nelson, R. D.; Gottlieb, D. J.; Balasubramanian, T. M.; Marshall, G. R. In *NIDA Research Monograph*; Rapaka, R. S., Barnett, G., Hawks, R. L., Eds.; U.S. Government Printing Office: Washington, DC, 1986; Vol. 69, pp 204–230.
- (37) Yang, Y. R.; Chiu, T. H.; Chen, C.-L. Structure-Activity Relationships of Naturally Occurring and Synthetic Opioid Tetrapeptides Acting on Locus Coeruleus Neurons. *Eur. J. Pharmacol.* **1999**, *372*, 229–236.
- (38) Santagada, V.; Caliendo, G.; Severino, B.; Perissutti, E.; Ceccarelli, F.; Giusti, L.; Mazzoni, M. R.; Salvatori, P. A. Probing the Shape of a Hydrophobic Pocket in the Active Site of  $\delta$ -Opioid Antagonists. *J. Pept. Sci.* **2001**, *7*, 374–385.
- (39) Lowry, O. H.; Rosebrough, N. J.; Farr, A.; Randall, R. J. Protein Measurement with Folin Phenol Reagent. *J. Biol. Chem.* **1951**, *193*, 265–275.
- (40) Cheng, Y. C.; Prusoff, W. H. Relationship between the Inhibition Constant ( $K_i$ ) and the Concentration of Inhibitor which Causes 50% Inhibition ( $\text{IC}_{50}$ ) of an Enzymatic Reaction. *Biochem Pharmacol.* **1973**, *22*, 3099–3108.
- (41) Koradi, R.; Billeter, M.; Wüthrich, K. MOLMOL: A Program for Display and Analysis of Macromolecular Structures. *J. Mol. Graphics* **1996**, *14*, 51–55.
- (42) Maple, J.; Dinur, U.; Hagler, A. T. Derivation of Force Fields for Molecular Mechanics and Dynamics from Ab Initio Energy Surface. *Proc. Natl. Acad. Sci. U.S.A.* **1988**, *85*, 5350–5354.
- (43) Hutchinson, E. G.; Thornton, J. M. PROMOTIF—A Program to Identify and Analyze Structural Motifs in Proteins. *Protein Sci.* **1996**, *5*, 212–220.

JM040867Y